

Research Article

Generalized Sparse Polarization Array for DOA Estimation Using Compressive Measurements

Tao Chen ¹, Jian Yang ^{1,2}, Weitong Wang ¹, and Muran Guo ¹

¹College of Information and Communication Engineering, Harbin Engineering University, Harbin 150001, China

²Beijing Institute of Remote Sensing Equipment, Beijing 100854, China

Correspondence should be addressed to Muran Guo; guomuran@hrbeu.edu.cn

Received 3 February 2021; Revised 24 February 2021; Accepted 11 March 2021; Published 31 March 2021

Academic Editor: Fangqing Wen

Copyright © 2021 Tao Chen et al. This is an open access article distributed under the Creative Commons Attribution License, which permits unrestricted use, distribution, and reproduction in any medium, provided the original work is properly cited.

The compressive array method, where a compression matrix is designed to reduce the dimension of the received signal vector, is an effective solution to obtain high estimation performance with low system complexity. While sparse arrays are often used to obtain higher degrees of freedom (DOFs), in this paper, an orthogonal dipole sparse array structure exploiting compressive measurements is proposed to estimate the direction of arrival (DOA) and polarization signal parameters jointly. Based on the proposed structure, we also propose an estimation algorithm using the compressed sensing (CS) method, where the DOAs are accurately estimated by the CS algorithm and the polarization parameters are obtained via the least-square method exploiting the previously estimated DOAs. Furthermore, the performance of the estimation of DOA and polarization parameters is explicitly discussed through the Cramér-Rao bound (CRB). The CRB expression for elevation angle and auxiliary polarization angle is derived to reveal the limit of estimation performance mathematically. The difference between the results given in this paper and the CRB results of other polarized reception structures is mainly due to the use of the compression matrix. Simulation results verify that, compared with the uncompressed structure, the proposed structure can achieve higher estimated performance with a given number of channels.

1. Introduction

In a traditional scalar sensor array, the time delay of the phased array is used to estimate the direction of arrival (DOA). In the practical application environment, however, the signal to be detected usually has certain polarization characteristics. The polarization sensitive array [1–3] can be used to obtain and utilize the spatial and polarization domain information of the signal source comprehensively, which lays a physical foundation for improving the overall performance of the array signal processing. Therefore, the concept of polarization is extended to wireless communication [4], radar systems [5], and many other fields of space science [6]. At present, the research on polarization parameter estimation mainly focuses on how to improve the estimation performance, such as estimation accuracy and degree of freedom (DOF). As the polarized state of a signal varies with polarization diversity, only if the polarization direction of a single antenna matches with the incoming wave, all energy of the incoming wave can be received; otherwise, the loss of

energy will occur [7]. Since a dual-polarized antenna [8, 9] can receive the signal energy along the horizontal and vertical branches, it can increase the receiving efficiency of signals.

To obtain a higher number of DOFs under the premise of a given number of sensors, sparse array structures [10–12] have been proposed under the coarray framework, which generate equivalent virtual array elements via extracting the correlation information of received signals. On the one hand, the nested array [11] can generate a difference coarray with all continuous lags, which is very useful for spatial smoothing-based estimation algorithms. However, since one subarray has the sensors placed with a half wavelength, the mutual coupling effects will compromise the estimation performance. In [13], a sparse nested array has been proposed, where the interelement spacing of the dense subarray is extended to suppress mutual coupling effects. The diversely polarized dipoles are used to further improve estimation performance. Moreover, the spatially spread orthogonal dipoles are exploited in the sparse nested array in [14], where a passive direction finding structure with high accuracy has been

proposed. Then, [15] further takes spatially spread square acoustic vector sensors into account, thus constructing a high-accuracy DOA estimation structure for an underdetermined case. On the other hand, the coprime array [12] can suppress the mutual coupling effect by using two sparse uniform linear arrays (ULA). In general, for a coprime array composed of an M -element subarray and an N -element subarray, up to $2M + N - 2$ uncorrelated sources can be distinguished. Therefore, the coprime array and its related improved structures [16] are also introduced into other radar structures [17]. In addition, [18] proposed an adaptive beamforming approach based on the coprime array, where the output performance is improved.

The DOA parameters, including the azimuth and elevation angle, are of great importance in many applications, especially the unmanned driving technology [19] which is one of the current hot research issues. Thus, different catalogs of DOA estimation methods have been proposed, for instance, the subspace methods [7], deep learning methods [20], and sparse reconstruction methods [21]. The compressive sensing (CS) theory is the kernel of sparse reconstruction methods. However, CS is first used in time domain to break through the limitation of the Nyquist Sampling Theorem [22], since a high sampling rate is usually required for wideband signals, thus leading to a high cost of analog-to-digital converters (ADCs). To be specific, if the number of nonzero elements in a vector is much less than that of the zero elements, then this vector is regarded as a sparse vector and can be recovered from a small sample set. Thus, the sampling rate is dramatically reduced. Then, as the polarization sensitive array develops, several DOA and polarization joint estimation algorithms have been proposed [23–25]. Moreover, in addition to the estimation algorithms, the CS has also been used in system design. The DOA estimation system exploiting compressive measurements can dramatically reduce the complexity and the computational burden. For example, the compressive measurement method has found many applications in the coprime arrays [26], one-bit quantization [27], modulated wideband converter [28], and MIMO radar [29].

Motivated by the above facts, in this paper, we mainly consider the orthogonal dipole antennas and propose a compressive measurement-based orthogonal dipole sparse array structure for the joint estimation of signal parameters. It is worth noting that there is no demand on the receive array structure, meaning that all kinds of dipole sparse array can be used. Based on the proposed structure, we first estimate the DOAs using a CS-based approach, and then the estimated DOAs are utilized to analyze the polarization parameters by a least-square estimation approach. In [24], the CS-based joint estimation of DOA and polarization parameters is proposed using a sparse array consisting of dual-polarized antenna elements. However, we would like to emphasize the contribution of this paper, as well as the difference with [24]:

- (a) In this paper, a two-dimensional polarization signal model is established, in which the azimuth angle and elevation angle are both taken into account,

while [24] only considers the one-dimensional case, that is, only the azimuth angle is included in the signal model. In addition, it should be noted that a steering vector matrix $\psi(\theta_k, \phi_k, \gamma_k, \eta_k)$ is introduced into the signal model to describe the coherent structure in the polarizational and spatial domains

- (b) The compression measurement method is applied to the proposed structure to compress the signal dimension by introducing a compression matrix Φ , therefore effectively reducing the number of channels required for subsequent digitization operations
- (c) Considering that the Cramér-Rao bound (CRB) indicates the lower bound of the estimation error for an unbiased system, we first derive the CRB expression for the elevation angle and auxiliary polarization angle of the proposed structure. Then, theoretical performance analysis and simulation verification are made via the CRB expression in this paper

Note that we use the CS theory twice in this paper. One is in the system design part, in order to reduce the dimension of received signal vector. The other is in the DOA estimation algorithm, where the group sparsity is used to obtain an improved number of DOF. Using the proposed structure, the number of channels is effectively controlled, thus reducing the hardware cost. In addition, although the compression leads to a degradation on the estimation performance, the proposed structure still outperforms the conventional dipole sparse array with the same number of channels, which can be clearly observed from both the theoretical derived CRB expression and the experimentally obtained root mean square error (RMSE). Therefore, the proposed structure also provides a flexible alternative option for low complexity polarization sensitive array with a relatively high estimation performance. Numerical simulations are conducted to examine the performance of the proposed structure.

The following of this paper is organized as follows: In Section 2, we build the system model of the proposed structure. Then, a CS-based algorithm is proposed in Section 3 to jointly estimate the DOAs and polarization parameters. In Section 4, the CRB expression for the estimation of DOAs and polarization parameters of the proposed structure is derived. Numerical simulation results are shown in Section 5, where the corresponding analysis is given simultaneously. Finally, Section 6 concludes the whole paper.

2. System Model of the Proposed Structure

First, we would like to briefly review the receiving model of the polarization signals. Polarization sensitive receive array is composed of L orthogonal dipoles, each of which is aligned with the y -axis in the Cartesian coordinate system. For the sake of convenience, the set $\mathbb{S} = \{d_{y1}, d_{y2}, \dots, d_{yL}\}$ is used to represent the positions of the sensors arranged in ascending order, and the antenna at the origin is assumed to be the reference, i.e., $d_{y1} = 0$. It is noted that the sensors can be sparsely placed. For instance, the sensors can be arranged as an

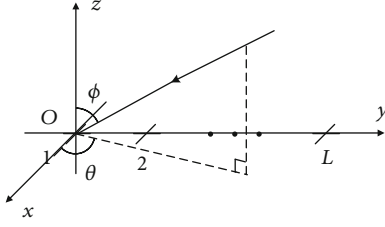


FIGURE 1: Schematic diagram of electromagnetic wave propagation.

extended coprime array according to set $\mathbb{S} = \{(Bad, 0 \leq a \leq 2A - 1) \cup (Abd, 0 \leq b \leq B - 1)\}$, where A and B are a pair of coprime integers. As shown in Figure 1, the signal from each dipole is processed separately; therefore, the array is divided into two subarrays according to the polarization receiving direction of the dipole:

- All dipoles pointing in the direction of the x -axis constitute *Subarray 1*
- All dipoles pointing in the direction of the y -axis constitute *Subarray 2*

Assume K narrow-band transverse electromagnetic (TEM) waves impinge upon the polarization sensitive array from the azimuth angle θ_k and elevation angle ϕ_k , where $\theta_k \in [0, \pi]$ and $\phi_k \in [-2/\pi, 2/\pi]$. It is assumed that each signal has an arbitrary elliptical electromagnetic polarization. The polarization of a TEM wave is often specified by two real parameters, namely, the auxiliary polarization angle γ_k ($\gamma_k \in [0, \pi/2]$) and the polarization phase difference η_k ($\eta_k \in [-\pi, \pi]$). The signal vector received by the polarization sensitive array, which has the dimension of $L_o = 2L$, is expressed as

$$\begin{aligned} \mathbf{x}(t) &= \sum_{k=1}^K [\psi(\theta_k, \phi_k, \gamma_k, \eta_k) \otimes \mathbf{u}(\theta_k, \phi_k)] \mathbf{s}_k(t) + \mathbf{n}(t) \\ &= \mathbf{A}\mathbf{s}(t) + \mathbf{n}(t), \end{aligned} \quad (1)$$

where we use \otimes to denote the Kronecker product. Denote $\mathbf{u}(\theta_k, \phi_k)$ as the L -dimensional spatial steering vector of the k th signal, expressed as

$$\mathbf{u}(\theta_k, \phi_k) = \left[e^{\frac{j2\pi d_{y1} \sin \theta_k \sin \phi_k}{\lambda}}, \dots, e^{\frac{j2\pi d_{yL} \sin \theta_k \sin \phi_k}{\lambda}} \right]^T, \quad (2)$$

in which λ is the signal wavelength. For simplicity of notation, we denote $\mathbf{u}(\theta_k, \phi_k)$ as \mathbf{u}_k . A vector matrix $\psi(\theta_k, \phi_k, \gamma_k, \eta_k)$ which describes the polarization information of incoming signals is defined as follows:

$$\psi(\theta_k, \phi_k, \gamma_k, \eta_k) = \psi_k = \Xi_{\theta_k, \phi_k} \mathbf{h}_{\gamma_k, \eta_k}, \quad (3)$$

where Ξ and \mathbf{h} are defined as

$$\begin{aligned} \Xi_{\theta_k, \phi_k} &= \begin{bmatrix} -\sin \theta_k & \cos \phi_k \cos \theta_k \\ \cos \theta_k & \cos \phi_k \sin \theta_k \end{bmatrix}, \\ \mathbf{h}_{\gamma_k, \eta_k} &= \begin{bmatrix} \cos \gamma_k \\ \sin \gamma_k e^{j\eta_k} \end{bmatrix}, \end{aligned} \quad (4)$$

respectively. Thus, $\mathbf{A} = [\psi_1 \otimes \mathbf{u}_1, \psi_2 \otimes \mathbf{u}_2, \dots, \psi_K \otimes \mathbf{u}_K]$ is the manifold matrix of polarization received signal, and $\mathbf{s}(t) = [s_1(t), s_2(t), \dots, s_K(t)]^T$ is the complex envelope. Noise vector $\mathbf{n}(t)$ is assumed to be the zero mean complex Gaussian processes, where each of its entries is statistically independent.

Then, let $\mathbf{x}_1(t)$ be the signal received on *Subarray 1* and $\mathbf{x}_2(t)$ the signal received on *Subarray 2*. Then, replace $\psi_k(1)$ and $\psi_k(2)$ with ψ_{xk} and ψ_{yk} , respectively. The received signal vector of subarrays are expressed as

$$\begin{aligned} \mathbf{x}_1(t) &= \sum_{k=1}^K [\psi_{xk} \otimes \mathbf{u}_k] s_k(t) + \mathbf{n}_1(t) = \mathbf{A}_1 \mathbf{s}(t) + \mathbf{n}_1(t), \\ \mathbf{x}_2(t) &= \sum_{k=1}^K [\psi_{yk} \otimes \mathbf{u}_k] s_k(t) + \mathbf{n}_2(t) = \mathbf{A}_2 \mathbf{s}(t) + \mathbf{n}_2(t). \end{aligned} \quad (5)$$

The proposed orthogonal dipole sparse array structure exploiting compressive measurements method is shown in Figure 2. The core principle of the compressive measurement method is to insert a combining network consisting of phase shifters and accumulators at the antenna outputs before subsequent digitization operations, which is equivalent to introducing a compression matrix $\Phi \in \mathbb{C}^{M \times L}$ ($M < L$) for linear operations mathematically. In this way, the received signal vector in the L -dimension is compressed to M -dimension and then output for subsequent signal processing [30].

It should be noted that the entries in the compression matrix are usually randomly selected from independent identically distributed parameters, and it is assumed that no additional noise is introduced during the compression process. In order to avoid information loss caused by data compression, the compression matrix can be optimized by various methods [27, 31, 32]. In this paper, Φ is selected to satisfy row-orthonormal, namely, $\Phi \Phi^H = \mathbf{I}_M$.

Then, the received signal vector of each subarray after compression is expressed as

$$\begin{aligned} \mathbf{y}_1(t) &= \Phi \left[\sum_{k=1}^K \mathbf{u}_k \psi_{xk} s_k(t) + \mathbf{n}_1(t) \right] = \bar{\mathbf{A}}_1 \mathbf{s}(t) + \bar{\mathbf{n}}_1(t), \\ \mathbf{y}_2(t) &= \Phi \left[\sum_{k=1}^K \mathbf{u}_k \psi_{yk} s_k(t) + \mathbf{n}_2(t) \right] = \bar{\mathbf{A}}_2 \mathbf{s}(t) + \bar{\mathbf{n}}_2(t). \end{aligned} \quad (6)$$

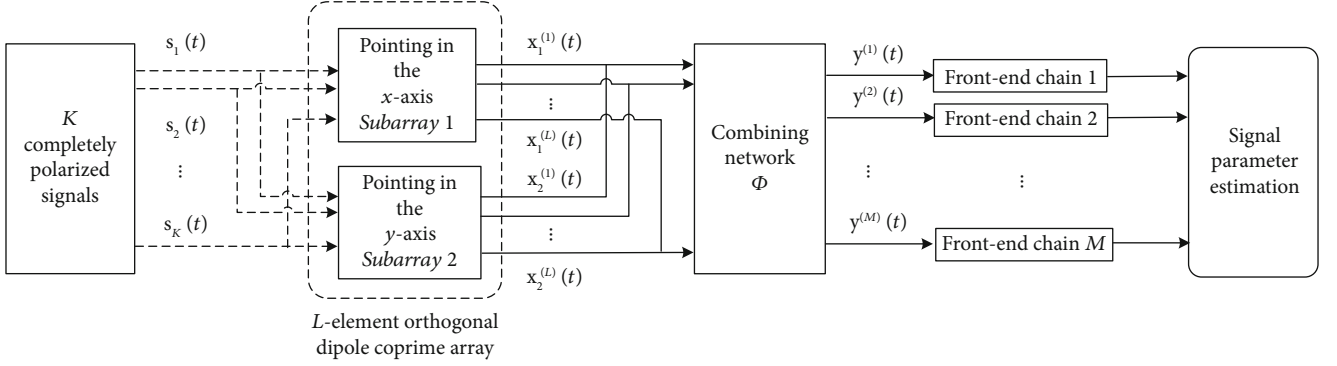


FIGURE 2: System model of the proposed compressive measurement-based orthogonal dipole sparse array structure.

Stacking the received vectors into a column vector yields

$$\mathbf{y}(t) = \tilde{\mathbf{A}}\mathbf{s}(t) + \tilde{\mathbf{n}}(t), \quad (7)$$

where $\mathbf{y}(t) = [\mathbf{y}_1^T(t), \mathbf{y}_2^T(t)]^T$ and $\tilde{\mathbf{A}} = [\tilde{\mathbf{A}}_1^T, \tilde{\mathbf{A}}_2^T]^T$ is the steering vector after compression with the k th term being

$$\tilde{\mathbf{a}}_k = \psi_k \otimes \tilde{\mathbf{u}}_k = [\psi_{xk}, \psi_{yk}]^T \otimes [\Phi \mathbf{u}_k]. \quad (8)$$

In addition, $\tilde{\mathbf{n}} = [\tilde{\mathbf{n}}_1^T(t), \tilde{\mathbf{n}}_2^T(t)]^T$ is the noise vector after compression.

Therefore, for the proposed structure, the length of the compressive received signal vector is $2M$, while the length of conventional sparse dipole array with the same configuration is $2L$. Assume that the number of snapshots is T . When the signal snapshots are used to compute the covariance matrix, the computational complexity of the proposed structure is $\mathcal{O}(4TM^2)$, while that of the conventional sparse dipole array is $\mathcal{O}(4TL^2)$.

3. Signal Parameter Estimation Approach

Since two-dimensional DOA estimation based on linear array cannot be realized, it is generally assumed that the signals and the linear array are in the yz plane, that is, the azimuth angle $\theta_k = \pi/2$. To avoid three-dimensional parameters, we search for ϕ_k , γ_k , and η_k ; [24] proposed a different reformulation, where a CS-based approach is first used to estimate the DOAs, and then the polarization parameters are estimated utilizing the estimated DOAs and a least-square estimation approach. In this paper, the above method is improved and applied to the proposed structure.

We start with the array output covariance matrix $\mathbf{R}_{yy} = E[\mathbf{y}(t)\mathbf{y}^H(t)]$. The self-lag covariance matrix for the data vector $\mathbf{y}^{(i)}(t)$ and the cross-lag covariance matrix between $\mathbf{y}^{(i)}(t)$ and $\mathbf{y}^{(j)}(t)$ can be obtained as

$$\mathbf{R}_{yy}^{(i)} = \Phi(\mathbf{U}\psi(i)\mathbf{R}_{ss}\psi(i)^H\mathbf{U}^H + p_n\mathbf{I}_L)\Phi^H,$$

$$\mathbf{R}_{yy}^{(i,j)} = \Phi\mathbf{U}\psi(i)\mathbf{R}_{ss}\psi(j)^H\mathbf{U}^H\Phi^H, \quad (9)$$

respectively ($1 \leq i \neq j \leq 2$), with \mathbf{R}_{ss} representing the source covariance matrix and p_n indicating the noise power. In addition, $\mathbf{U} = [\mathbf{u}_1, \mathbf{u}_2, \dots, \mathbf{u}_K]$ is a spatial phase matrix with $L \times K$ dimension.

We denote the vectorized form of \mathbf{R}_{yy} as \mathbf{r}_{yy} , which can be regarded as a received data vector at a virtual array with an extended coarray aperture. On the basis of the matrix algorithm, the vectorization covariance matrix of different subarrays are calculated as

$$\mathbf{r}_{yy}^{(i)} = \Phi_0 \left[(\mathbf{U}^* \odot \mathbf{U}) \text{vec}(\psi(i)\mathbf{R}_{ss}\psi(i)^H) + p_n \tilde{\mathbf{I}}_{L^2} \right],$$

$$\mathbf{r}_{yy}^{(i,j)} = \Phi_0 (\mathbf{U}^* \odot \mathbf{U}) \text{vec}(\psi(i)\mathbf{R}_{ss}\psi(j)^H), \quad (10)$$

in which we denote $(\Phi^* \otimes \Phi) \in \mathbb{C}^{M^2 \times L^2}$ as Φ_0 for notational simplicity. A matrix $\mathbf{U}^* \odot \mathbf{U} = [\mathbf{u}_1^* \otimes \mathbf{u}_1, \dots, \mathbf{u}_K^* \otimes \mathbf{u}_K]$ that leads to a series of virtual array elements is defined, and the Khatri-Rao product is denoted by \odot . Define a set of integers $\mathbb{D} = \{d_{y\alpha} - d_{y\beta} | d_{y\alpha}, d_{y\beta} \in \mathbb{S}\}$ to represent the locations of virtual sensors and arrange them in ascending order. Then, the corresponding array manifold can be represented as $\mathbf{U}_{\mathbb{D}} = [\mathbf{u}_{\mathbb{D}1}, \mathbf{u}_{\mathbb{D}2}, \dots, \mathbf{u}_{\mathbb{D}K}]$.

The vectorized covariance matrices are stacked and simplified as

$$\begin{bmatrix} \mathbf{r}_{yy}^{(1)} \\ \mathbf{r}_{yy}^{(1,2)} \\ \mathbf{r}_{yy}^{(2,1)} \\ \mathbf{r}_{yy}^{(2)} \end{bmatrix} = \begin{bmatrix} \Phi_0(\mathbf{U}^* \odot \mathbf{U})\mathbf{p}^{(1)} \\ \Phi_0(\mathbf{U}^* \odot \mathbf{U})\mathbf{p}^{(1,2)} \\ \Phi_0(\mathbf{U}^* \odot \mathbf{U})\mathbf{p}^{(2,1)} \\ \Phi_0(\mathbf{U}^* \odot \mathbf{U})\mathbf{p}^{(2)} \end{bmatrix} + \begin{bmatrix} p_n \Phi_0 \tilde{\mathbf{I}}_{L^2} \\ 0 \\ 0 \\ p_n \Phi_0 \tilde{\mathbf{I}}_{L^2} \end{bmatrix}, \quad (11)$$

where $\tilde{\mathbf{I}}_{L^2} = \text{vec}(\mathbf{I}_L)$ and the k -th item containing signal power is represented as

$$\mathbf{p}_k^{(1)} = p_k (\cos \gamma_k)^2, \quad (12)$$

$$\mathbf{p}_k^{(2)} = p_k (\cos \phi_k \sin \gamma_k)^2, \quad (13)$$

$$\mathbf{p}_k^{(1,2)} = -p_k \cos \phi_k \sin \gamma_k \cos \gamma_k e^{-j\eta_k}, \quad (14)$$

$$\mathbf{p}_k^{(2,1)} = p_k \cos \phi_k \sin \gamma_k \cos \gamma_k e^{j\eta_k}. \quad (15)$$

Discretizing the spatial domain $\Omega_{P,Q}$ ($P, Q \gg K$) into a grid, let $\mathbf{d}_{\text{grid}}(\theta_p, \phi_q)$ ($1 \leq p \leq P, 1 \leq q \leq Q$) represent the steering vector. Thus, the discretized array manifold corresponding to this grid can be obtained as

$$\mathbf{G}_{\text{grid},i} = \Phi_0 \left[\mathbf{d}_{\text{grid}}^*(\theta_1, \phi_1) \otimes \mathbf{d}_{\text{grid}}(\theta_1, \phi_1), \dots, \mathbf{d}_{\text{grid}}^*(\theta_P, \phi_Q) \otimes \mathbf{d}_{\text{grid}}(\theta_P, \phi_Q) \right]. \quad (16)$$

It can be known that there is a γ_k ($k \in [1, K]$) such that $\sin \gamma_k \rightarrow 0$ or $\cos \gamma_k \rightarrow 0$. In this case, $\mathbf{p}^{(1,2)}$ and $\mathbf{p}^{(2,1)}$ approach zero simultaneously due to the item $\sin \gamma_k \cos \gamma_k$. Thus, using $\mathbf{p}^{(1,2)}$ and $\mathbf{p}^{(2,1)}$ has no improvement on the estimation performance. Meanwhile, the computational complexity is increased. However, it is impossible for $(\cos \gamma_k)^2$ and $(\sin \gamma_k)^2$ to be equal to zero at the same time. Thus, both $\mathbf{p}^{(1)}$ and $\mathbf{p}^{(2)}$ can be utilized for DOA estimation, and we have

$$\mathbf{r} = \tilde{\mathbf{G}}_{\text{grid}} \mathbf{p} + p_n \tilde{\mathbf{I}} = \tilde{\mathbf{G}} \tilde{\mathbf{p}}, \quad (17)$$

where $\mathbf{r} = [(\mathbf{r}_{yy}^{(1)})^T, (\mathbf{r}_{yy}^{(2)})^T]^T$, $\mathbf{p} = [(\mathbf{p}^{(1)})^T, (\mathbf{p}^{(2)})^T]^T$, $\tilde{\mathbf{I}} = \text{diag}\{\Phi_0 \text{vec}(\mathbf{I}_L), \Phi_0 \text{vec}(\mathbf{I}_L)\}$, and $\tilde{\mathbf{G}}_{\text{grid}} = \text{diag}\{\mathbf{G}_{\text{grid},1}, \mathbf{G}_{\text{grid},2}\}$. The nonzero entries of $\mathbf{p}^{(1)}$ and $\mathbf{p}^{(2)}$ share the same support corresponding to the same grid. Thus, to utilize the group sparsity, hereby we define a sparse vector $\xi(\tilde{\mathbf{p}})$ as the ℓ_2 -norm of each row in the matrix $[\mathbf{p}^{(1)}, \mathbf{p}^{(2)}]$. The group LASSO algorithm [21] is utilized to solve the group sparsity problem, and the minimization problem is as follows:

$$\hat{\tilde{\mathbf{p}}} = \underset{\tilde{\mathbf{p}}}{\text{argmin}} \frac{1}{2} \|\mathbf{r} - \tilde{\mathbf{G}}_{\text{grid}} \tilde{\mathbf{p}}\|_2 + \mu_0 \|\xi(\tilde{\mathbf{p}})\|_1. \quad (18)$$

The nonzero items in $\hat{\tilde{\mathbf{p}}}$ at its respective positions are the estimated DOAs.

The estimated elevation angle is denoted as $\hat{\phi} = [\hat{\phi}_1, \dots, \hat{\phi}_K]^T$, and the estimation of the array manifold is defined as $\hat{\mathbf{G}} = \mathbf{G}_{\text{grid}} \in \mathbb{C}^{M^2 \times K}$, which is used for the next polarization parameter estimation. Then, the vectors $\mathbf{p}^{(1)}$, $\mathbf{p}^{(1,2)}$, $\mathbf{p}^{(2,1)}$, and $\mathbf{p}^{(2)}$ which contain the polarization parameters can be obtained using the following least-square estimation:

$$\hat{\mathbf{p}}^{(i,j)} = \left[\hat{\mathbf{G}}^H \hat{\mathbf{G}} \right]^{-1} \hat{\mathbf{G}}^H \mathbf{r}^{(i,j)}, \quad i, j = 1, 2, \quad (19)$$

where the k th item is expressed in (12)–(15). Simplifying the above equations, we have the following equations:

$$\cos(2\gamma_k) = \frac{\hat{\mathbf{p}}_k^{(1)} - \left(\hat{\mathbf{p}}_k^{(2)} / (\cos \hat{\phi}_k)^2 \right)}{p_k}, \quad (20)$$

$$\cos(\eta_k) \sin(2\gamma_k) = \frac{\hat{\mathbf{p}}_k^{(2,1)} - \hat{\mathbf{p}}_k^{(1,2)}}{p_k \cos \hat{\phi}_k}.$$

The estimated polarization phase difference $\hat{\eta}_k$ can be obtained by expressing $\sin(2\gamma_k)$ in terms of $\cos(2\gamma_k)$, whereas the estimated auxiliary polarization angle can be calculated by the following equation:

$$\hat{\gamma}_k = \frac{1}{2} \text{atan2} \left\{ \left| \hat{\mathbf{p}}_k^{(2)} / \hat{\mathbf{p}}_k^{(1)} \right|^{1/2}, \cos \hat{\phi}_k \right\}. \quad (21)$$

Thus, the joint estimation of DOA and polarization parameters is completed. The procedure of the proposed algorithm is summarized in Algorithm 1.

4. The Cramér-Rao Bound Analysis

Since the linear array is exploited, without loss of generality, the azimuth angle θ_k and polarization phase difference η_k are set as $\pi/2$, thus limiting the DOAs to the yz plane and the polarization state to the same great circle orbit of Poincare sphere. The CRB [33] provides a lower bound on the covariance matrix of any unbiased estimator. In fact, under mild regularity conditions, the maximum likelihood estimator achieves the CRB asymptotically, as the number of snapshots tends to infinity. Given T independent samples of a zero mean Gaussian process $\mathbf{y}(t)$ whose statistics depend on a parameter vector α

$$\alpha = \left[\Omega^T, Y^T, \mathbf{p}^T, p_n^{(1)}, p_n^{(2)} \right]^T, \quad (22)$$

with $\Omega = [\phi_1, \phi_2, \dots, \phi_K]^T$, $Y = [\gamma_1, \gamma_2, \dots, \gamma_K]^T$, and $\mathbf{p} = [p_1, p_2, \dots, p_K]^T$, the CRB is obtained by the inverse of the Fisher informative matrix (FIM) [34].

$$\text{CRB}(\alpha) = \frac{1}{T} (\mathbf{G}^H \mathbf{\Pi} \mathbf{G})^{-1}, \quad (23)$$

in which

$$\mathbf{G} = \mathbf{M} \begin{bmatrix} \frac{\partial \mathbf{r}_{yy}}{\partial \phi_1}, \dots, \frac{\partial \mathbf{r}_{yy}}{\partial \phi_K}, \frac{\partial \mathbf{r}_{yy}}{\partial \gamma_1}, \dots, \frac{\partial \mathbf{r}_{yy}}{\partial \gamma_K} \end{bmatrix}, \quad (24)$$

$$\mathbf{\Delta} = \mathbf{M} \begin{bmatrix} \frac{\partial \mathbf{r}_{yy}}{\partial p_1}, \dots, \frac{\partial \mathbf{r}_{yy}}{\partial p_K}, \frac{\partial \mathbf{r}_{yy}}{\partial p_n^{(1)}}, \frac{\partial \mathbf{r}_{yy}}{\partial p_n^{(2)}} \end{bmatrix}, \quad (25)$$

and $\mathbf{M} = (\mathbf{R}_{yy}^T \otimes \mathbf{R}_{yy})^{-1/2}$.


```

procedure polarization signal parameter estimation
  Initialize  $\mathbf{r}_{yy}^{(i)} \leftarrow \text{vec}(\mathbf{R}_{yy}^{(i)})$ ,  $\mathbf{r}_{yy}^{(i,j)} \leftarrow \text{vec}(\mathbf{R}_{yy}^{(i,j)})$ 
  for  $(\theta_p, \phi_q)$ ,  $1 \leq p \leq P$ ,  $1 \leq q \leq Q$  do
     $\hat{\mathbf{G}}_{\text{grid}} \leftarrow \Phi_0[\mathbf{d}_{\text{grid}}^*(\theta_1, \phi_1) \otimes \mathbf{d}_{\text{grid}}(\theta_1, \phi_1), \dots, \mathbf{d}_{\text{grid}}^*(\theta_P, \phi_Q) \otimes \mathbf{d}_{\text{grid}}(\theta_P, \phi_Q)]$ 
     $\hat{\mathbf{p}} \leftarrow \underset{\mathbf{p}}{\text{argmin}} 1/2 \|\mathbf{r} - \hat{\mathbf{G}}_{\text{grid}} \mathbf{p}\|_2 + \mu_0 \|\xi(\hat{\mathbf{p}})\|_1$ 
  end
  if  $\hat{\mathbf{p}}_i \neq 0$ ,  $i \in [1, Q]$ 
    then  $\hat{\phi}_k \leftarrow$  the position of  $\hat{\mathbf{p}}_i$ ,  $k = 1, \dots, K$ 
  end
  for  $\hat{\phi}_k \in [\hat{\phi}_1, \dots, \hat{\phi}_K]$ ,  $p_k \in [p_1, \dots, p_K]$  do
     $\cos(2\gamma_k) \leftarrow \hat{\mathbf{p}}_k^{(1)} - (\hat{\mathbf{p}}_k^{(2)} / (\cos \hat{\phi}_k)^2) / p_k$ 
     $\cos(\eta_k) \sin(2\gamma_k) \leftarrow \hat{\mathbf{p}}_k^{(2,1)} - \hat{\mathbf{p}}_k^{(1,2)} / p_k \cos \hat{\phi}_k$ 
     $\hat{\gamma}_k \leftarrow 1/2 \text{atan2}\{|\hat{\mathbf{p}}_k^{(2)} / \hat{\mathbf{p}}_k^{(1)}|^{1/2}, \cos \hat{\phi}_k\}$ 
  end
  return  $\hat{\phi} \leftarrow [\hat{\phi}_1, \dots, \hat{\phi}_K]^T$ ,  $\hat{\eta} \leftarrow [\hat{\eta}_1, \dots, \hat{\eta}_K]^T$ ,  $\hat{\gamma} \leftarrow [\hat{\gamma}_1, \dots, \hat{\gamma}_K]^T$ 
end procedure

```

ALGORITHM 1: Procedure of the proposed algorithm.

Then, denote $\text{diag}\{\Phi, \Phi\}$ as $\Psi \in \mathbb{C}^{2M \times 2L}$, and vectorizing \mathbf{R}_{yy} yields

$$\mathbf{r}_{yy} = (\tilde{\mathbf{A}}^* \otimes \tilde{\mathbf{A}}) \text{vec}(\mathbf{R}_{ss}) + \text{vec}(\mathbf{R}_{nn}). \quad (26)$$

Expand $(\tilde{\mathbf{A}}^* \otimes \tilde{\mathbf{A}})$ as $\sum_{k=1}^K [(\psi_k \otimes \tilde{\mathbf{u}}_k)^* \otimes (\psi_k \otimes \tilde{\mathbf{u}}_k)]$, so that the \mathbf{r}_{yy} is finally simplified to the following form due to space limitation:

$$\mathbf{r}_{yy} = \sum_{k=1}^K \mathbf{V}_0 \mathbf{H}_k \Gamma_k \mathbf{J} \mathbf{u}_{\mathbb{D}k} p_k + \mathbf{V}_0 p_n \text{vec}(\mathbf{I}_{L_o}). \quad (27)$$

Several definitions are given to illustrate the vectorized results in (27):

$$\begin{aligned} \mathbf{V}_0 &= \Psi^* \otimes \Psi, \\ \mathbf{H}_k &= \begin{bmatrix} \mathbf{h}_k^*(1) \mathbf{I}_L & & \\ & \mathbf{h}_k^*(2) \mathbf{I}_L & \\ & & \mathbf{h}_k^*(3) \mathbf{I}_L \end{bmatrix} \otimes \begin{bmatrix} \mathbf{h}_k(1) \mathbf{I}_L & & \\ & \mathbf{h}_k(2) \mathbf{I}_L & \\ & & \mathbf{h}_k(3) \mathbf{I}_L \end{bmatrix}, \\ \Gamma_k &= \begin{bmatrix} -\mathbf{I}_L & \\ \cos \phi_k \mathbf{I}_L & \end{bmatrix} \otimes \begin{bmatrix} -\mathbf{I}_L & \\ \cos \phi_k \mathbf{I}_L & \end{bmatrix}. \end{aligned} \quad (28)$$

Besides, the binary matrix \mathbf{J} has the definition as follows:

$$\langle \mathbf{J} \rangle_{:,d} = \text{vec}(\mathbf{I}(d)), \quad d \in \mathbb{D}, \quad (29)$$

where $\mathbf{I}(d)$ satisfies

$$\langle \mathbf{I}(d) \rangle_{a,b} = \begin{cases} 1, & \text{if } a - b = d, \\ 0, & \text{otherwise.} \end{cases} \quad (30)$$

Thus, by utilizing the relationship $\mathbf{u}_k^* \otimes \mathbf{u}_k = \mathbf{J} \mathbf{u}_{\mathbb{D}k}$, \mathbf{u}_k and $\mathbf{u}_{\mathbb{D}k}$ can be bridged.

Taking the derivatives of \mathbf{r}_{yy} with respect to the DOA, polarization, signal power, and noise power, we have following results:

$$\frac{\partial \mathbf{r}_{yy}}{\partial \phi_k} = 2 \mathbf{V}_0 \mathbf{H}_k \Gamma_k' \mathbf{J} \mathbf{u}_k p_k + j\pi \mathbf{V}_0 \mathbf{H}_k \Gamma_k \mathbf{J} \text{diag}(\mathbb{D}) \cos \phi_k \mathbf{u}_k p_k, \quad (31)$$

$$\frac{\partial \mathbf{r}_{yy}}{\partial \gamma_k} = \mathbf{V}_0 \left[\mathbf{H}'_k + (\mathbf{H}'_k)^* \right] \Gamma_k \mathbf{J} \mathbf{u}_k p_k, \quad (32)$$

$$\frac{\partial \mathbf{r}_{yy}}{\partial p_k} = \mathbf{V}_0 \mathbf{H}_k \Gamma_k \mathbf{J} \mathbf{u}_k, \quad (33)$$

$$\frac{\partial \mathbf{r}_{yy}}{\partial p_n^{(1)}} = \mathbf{V}_0 \text{vec} \left(\begin{bmatrix} \mathbf{I}_L & 0 \\ 0 & 0 \end{bmatrix} \right), \quad \frac{\partial \mathbf{r}_{yy}}{\partial p_n^{(2)}} = \mathbf{V}_0 \text{vec} \left(\begin{bmatrix} 0 & 0 \\ 0 & \mathbf{I}_L \end{bmatrix} \right), \quad (34)$$

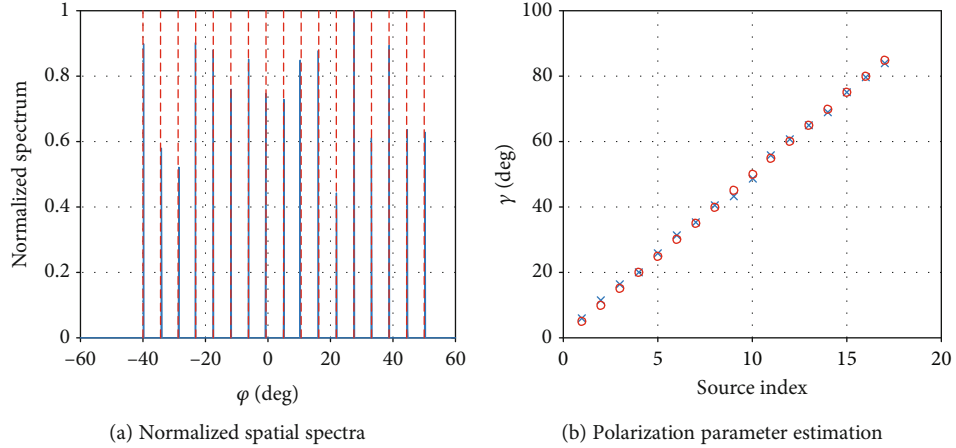


FIGURE 3: Signal parameter estimation of the proposed structure (SNR = 5 dB and 1,000 snapshots).

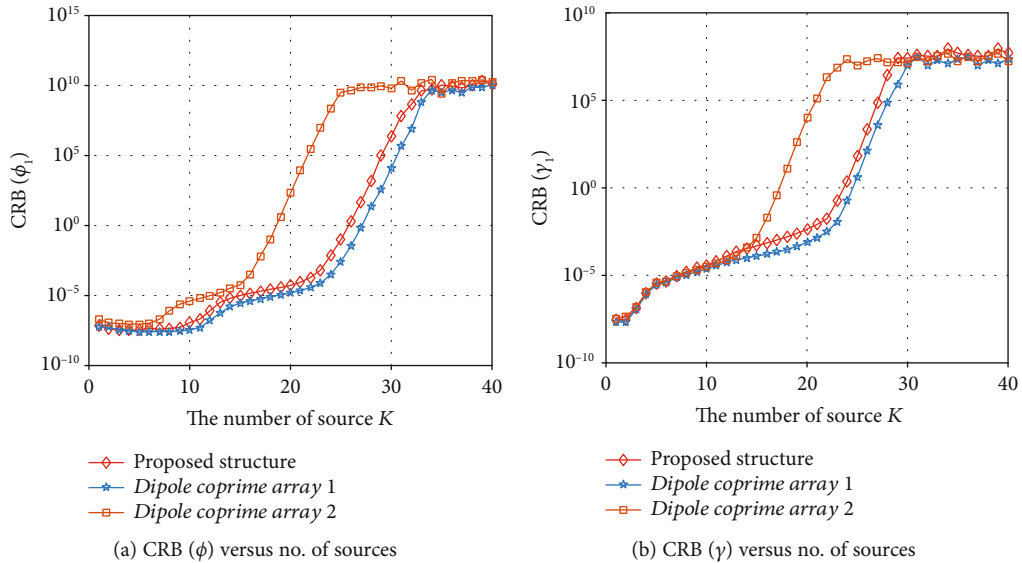


FIGURE 4: CRB versus the number of sources (SNR = 10 dB and 1,000 snapshots).

where

$$\mathbf{I}'_k = \begin{bmatrix} \mathbf{0} \\ -\sin \phi_k \mathbf{I}_L \end{bmatrix} \otimes \begin{bmatrix} -\mathbf{I}_L \\ \cos \phi_k \mathbf{I}_L \end{bmatrix} + \begin{bmatrix} -\mathbf{I}_L \\ \cos \phi_k \mathbf{I}_L \end{bmatrix} \otimes \begin{bmatrix} \mathbf{0} \\ -\sin \phi_k \mathbf{I}_L \end{bmatrix},$$

$$\mathbf{H}'_k = - \begin{bmatrix} \sin \gamma_k \mathbf{I}_L \\ j \cos \gamma_k \mathbf{I}_L \end{bmatrix} \otimes \begin{bmatrix} \cos \gamma_k \mathbf{I}_L \\ j \sin \gamma_k \mathbf{I}_L \end{bmatrix}. \quad (35)$$

Substituting (31)–(34) into (23), (24), and (25) leads to the CRB for the proposed structure.

5. Simulation Results

Throughout our simulations, the 10-element coprime array with $A=3$ and $B=5$ is considered. Without additional instructions, we assume the channel number after compression is $M=8$, and $\Phi \in \mathbb{C}^{8 \times 10}$ is generated from the standard complex Gaussian distribution. The incident signal is generated uniformly in the range of $\phi_k \in [-40^\circ, 50^\circ]$ with $\theta_k = \pi/2$, and the auxiliary polarization angle and polarization phase difference are evenly distributed in $\gamma_k \in [5^\circ, 85^\circ]$ and $\eta_k \in [-120^\circ, 150^\circ]$. Under the condition that SNR = 5 dB and 1,000 snapshots, the elevation angle is estimated using the CS-based approach. The angle range from -60° to 60° is uniformly divided into grids with a 0.1° searching step.

The signal parameter estimation results of 17 sources using the proposed structure are shown in Figure 3, where the actual parameter values are marked in red. Compared with the results in [24], the proposed structure with channel number compression can still correctly analyze 17 signals

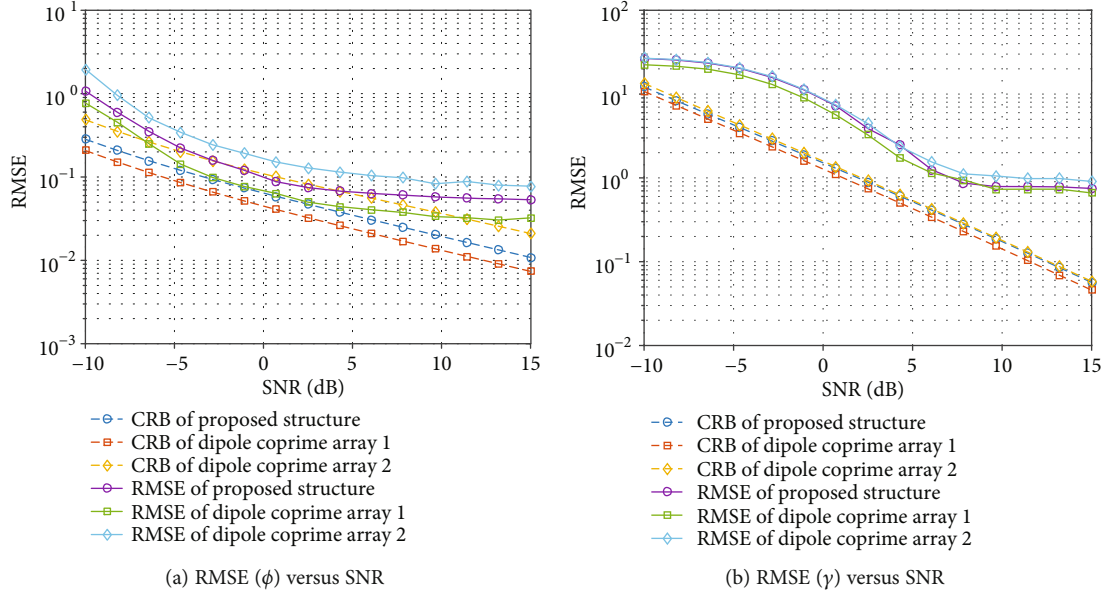


FIGURE 5: RMSE versus SNR (1,000 snapshots).

with 10 physical elements. Then, the variation of CRB derived with the number of sources is simulated to verify the DOF that the proposed structure can obtain. To further analyze the estimation performance of the proposed structure, the following coprime array configurations are considered as the comparison structure: (a) the proposed structure with $L = 10, M = 8$; (b) the 10-element coprime array with the compression matrix Φ is equal to a unit matrix, that is, without compression, denoted as *dipole coprime array 1*; and (c) the 8-element coprime array with $A = 2$ and $B = 5$, namely, $L = M = 8$, denoted as *dipole coprime array 2*, in which the idea of the CACIS configuration idea proposed in [35] is used for reference.

Figure 4 describes the CRB curves of ϕ and γ versus the number of sources when taking 1,000 snapshots at 10 dB SNR. When the compression ratio is $L/M = 1.25$, the DOFs obtained by the proposed structure is not much less than that obtained by an uncompressed structure with the same number of physical elements, namely, *dipole coprime array 1*. However, compared with *dipole coprime array 2* with the same number of channels, the proposed structure can resolve more uncorrelated signal sources, showing the superiority of the proposed structure for the number of DOFs.

The RMSE versus SNR of the comparison structure is shown in Figure 5. The CRB (ϕ) and CRB (γ) of the three array configurations are presented by dash lines. The order of RMSE depicted by solid lines is consistent with that of CRB shown in Figure 4. It can be observed in Figure 4 that the downward trend of the RMSE curves can also fit the CRB curves well, while in Figure 4, the RMSE curves tend to be flat as the SNR increases since the search step is limited by the RIP criterion. Due to the largest number of channels, the estimation accuracy of *dipole coprime array 1* is the highest among the three configurations, while the computational complexity is also the highest. In the case of the same number of channels, the proposed structure has a lower RMSE than

dipole coprime array 2. In general, from the perspective of the number of inequalities, dimensionality reduction can inevitably lead to a decrease in estimation performance, such as DOF and estimation accuracy. In order to achieve the purpose of avoiding excessive system complexity, better estimation performance can be obtained by using the proposed structure for DOA estimation, which also verifies our previous analysis. On the other hand, in Figure 4, it can be observed that, in a low SNR region, the performance of the proposed structure is almost the same as that of the *dipole coprime array 2*, indicating that the compressive measurement-based structure has no significant improvement on the estimation of polarization parameters. However, in a large SNR region, the accuracy of the proposed structure approaches the *dipole coprime array 1*. We must note that this improvement is mainly caused by limitation of the step of the searching grid. To be specific, as the SNR increases, the estimation performance achieves the ceiling of current searching step, thus leading to the phenomenon that the proposed structure has almost the same performance as *dipole coprime array 1*. Theoretically speaking, by observing the CRB curves shown in Figures 3 and 4, the improvement on the estimation of polarization parameters is negligible.

6. Conclusion

In this paper, we proposed a compressive measurement-based orthogonal dipole sparse array structure, which can be used for high-performance signal parameter estimation with a small number of given elements. In the joint estimation algorithm of DOA and polarization parameters, the CS-based algorithm and the least-square estimation method were adopted. Then, based on compressive measurements, we derived the CRB expression for the elevation angle and auxiliary polarization angle. By comparing to the array configurations with the unit matrix as the compression matrix, we

considered the CRB curves versus the number of independent signal sources and SNR. Thus, we come to the conclusion that, under the condition that we control the system complexity by reducing the number of channels, better parameter estimation performance can be obtained by the proposed orthogonal dipole array structure, especially for the estimation of DOAs. Simulation results also verified the theoretical analysis.

Data Availability

If data is needed, please contact M. Guo (email: guomur-an@hrbeu.edu.cn) for the code of numerical simulations.

Conflicts of Interest

The authors declare no conflict of interest.

Acknowledgments

This work was supported by the National Natural Science Foundation of China (grant numbers 62071137 and 62001136) and the Key Laboratory of Advanced Marine Communication and Information Technology.

References

- [1] V. H. Rumsey, G. A. Deschamps, M. L. Kales, J. I. Bohnert, and H. G. Booker, "Techniques for handling elliptically polarized waves with special reference to antennas: introduction," *Proceedings of the IRE*, vol. 39, no. 5, pp. 533-534, 1951.
- [2] W. Lee and Yu Yeh, "Polarization diversity system for mobile radio," *IEEE Transactions on Communications*, vol. 20, no. 5, pp. 912-923, 1972.
- [3] D. Giuli, "Polarization diversity in radars," *Proceedings of the IEEE*, vol. 74, no. 2, pp. 245-269, 1986.
- [4] R. G. Vaughan, "Polarization diversity in mobile communications," *IEEE Transactions on Vehicular Technology*, vol. 39, no. 3, pp. 177-186, 1990.
- [5] K. Ouchi, "Recent trend and advance of synthetic aperture radar with selected topics," *Remote Sensing*, vol. 5, no. 2, pp. 716-807, 2013.
- [6] E. H. Satorius, Z. Ye, and E. D. Archer, "Polarization combining scheme for radio direction finding with multipath," in *2001 MILCOM Proceedings Communications for Network-Centric Operations: Creating the Information Force (Cat. No. 01CH37277)*, vol. 1, pp. 383-387, McLean, VA, USA, 2001.
- [7] R. Schmidt, "Multiple emitter location and signal parameter estimation," *IEEE Transactions on Antennas and Propagation*, vol. 34, no. 3, pp. 276-280, 1986.
- [8] Y. Tian, X. Sun, and S. Zhao, "Sparse-reconstruction-based direction of arrival, polarisation and power estimation using a cross-dipole array," *IET Radar, Sonar and Navigation*, vol. 9, no. 6, pp. 727-731, 2015.
- [9] G. Zheng, "Two-dimensional DOA estimation for polarization sensitive array consisted of spatially spread crossed-dipole," *IEEE Sensors Journal*, vol. 18, no. 12, pp. 5014-5023, 2018.
- [10] A. Moffet, "Minimum-redundancy linear arrays," *IEEE Transactions on Antennas and Propagation*, vol. 16, no. 2, pp. 172-175, 1968.
- [11] P. Pal and P. P. Vaidyanathan, "Nested arrays: a novel approach to array processing with enhanced degrees of freedom," *IEEE Transactions on Signal Processing*, vol. 58, no. 8, pp. 4167-4181, 2010.
- [12] P. P. Vaidyanathan and P. Pal, "Sparse sensing with co-prime samplers and arrays," *IEEE Transactions on Signal Processing*, vol. 59, no. 2, pp. 573-586, 2011.
- [13] J. He, Z. Zhang, T. Shu, and W. Yu, "Sparse nested array with aperture extension for high accuracy angle estimation," *Signal Processing*, vol. 176, article 107700, 2020.
- [14] J. He, L. Li, and T. Shu, "Sparse nested arrays with spatially spread orthogonal dipoles: high accuracy passive direction finding with less mutual coupling," *IEEE Transactions on Aerospace and Electronic Systems*, 2021.
- [15] J. He, L. Li, and T. Shu, "Sparse nested arrays with spatially spread square acoustic vector sensors for high accuracy under-determined direction finding," *IEEE Transactions on Aerospace and Electronic Systems*, 2021.
- [16] C. Zhou, Y. Gu, X. Fan, Z. Shi, G. Mao, and Y. D. Zhang, "Direction-of-arrival estimation for coprime array via virtual array interpolation," *IEEE Transactions on Signal Processing*, vol. 66, no. 22, pp. 5956-5971, 2018.
- [17] Z. Zhang, C. Zhou, Y. Gu, J. Zhou, and Z. Shi, "An IDFT approach for coprime array direction-of-arrival estimation," *Digital Signal Processing*, vol. 94, pp. 45-55, 2019.
- [18] C. Zhou, Y. Gu, S. He, and Z. Shi, "A robust and efficient algorithm for coprime array adaptive beamforming," *IEEE Transactions on Vehicular Technology*, vol. 67, no. 2, pp. 1099-1112, 2018.
- [19] L. Wan, L. Sun, K. Liu, X. Wang, Q. Lin, and T. Zhu, "Autonomous vehicle source enumeration exploiting non-cooperative UAV in software defined internet of vehicles," *IEEE Transactions on Intelligent Transportation Systems*, pp. 1-13, 2020.
- [20] L. Wan, Y. Sun, L. Sun, Z. Ning, and J. J. P. C. Rodrigues, "Deep learning based autonomous vehicle super resolution DOA estimation for safety driving," *IEEE Transactions on Intelligent Transportation Systems*, pp. 1-15, 2020.
- [21] Y. D. Zhang, M. G. Amin, and B. Himed, "Sparsity-based DOA estimation using co-prime arrays," in *2013 IEEE International Conference on Acoustics, Speech and Signal Processing*, pp. 3967-3971, Vancouver, BC, Canada, 2013.
- [22] D. L. Donoho, "Compressed sensing," *IEEE Transactions on Information Theory*, vol. 52, no. 4, pp. 1289-1306, 2006.
- [23] J. Yang, T. Chen, L. Shi, and C. Zhang, "Joint DOA and polarization estimation based on multi-polarization sensitive array," in *International Conference in Communications, Signal Processing, and Systems*, Springer, Harbin, China, 2017.
- [24] B. K. Chalise, Y. D. Zhang, and B. Himed, "Compressed sensing based joint DOA and polarization angle estimation for sparse arrays with dual-polarized antennas," in *2018 IEEE Global Conference on Signal and Information Processing (GlobalSIP)*, pp. 251-255, Anaheim, CA, U. S, 2018.
- [25] L. Wan, K. Liu, Y.-C. Liang, and T. Zhu, "DOA and polarization estimation for non-circular signals in 3-D millimeter wave polarized massive MIMO systems," *IEEE Transactions on Wireless Communications*, 2021.
- [26] C. Zhou, Y. Gu, Y. D. Zhang, Z. Shi, T. Jin, and X. Wu, "Compressive sensing-based coprime array direction-of-arrival estimation," *IET Communications*, vol. 11, no. 11, pp. 1719-1724, 2017.
- [27] T. Chen, M. Guo, and X. Huang, "Direction finding using compressive one-bit measurements," *IEEE Access*, vol. 6, no. 1, pp. 41201-41211, 2018.

- [28] T. Chen, X. Han, and Y. Yu, "A sub-Nyquist sampling digital receiver system based on array compression," *Progress In Electromagnetics Research Letters*, vol. 88, pp. 21–28, 2020.
- [29] T. Chen, J. Yang, and M. Guo, "A MIMO radar-based DOA estimation structure using compressive measurements," *Sensors*, vol. 19, no. 21, 2019.
- [30] M. Guo, Y. D. Zhang, and T. Chen, "DOA estimation using compressed sparse array," *IEEE Transactions on Signal Processing*, vol. 66, no. 15, pp. 4133–4146, 2018.
- [31] M. Ibrahim, V. Ramireddy, A. Lavrenko et al., "Design and analysis of compressive antenna arrays for direction of arrival estimation," *Signal Processing*, vol. 138, no. 9, pp. 35–47, 2017.
- [32] Y. Gu, Y. D. Zhang, and N. A. Goodman, "Optimized compressive sensing-based direction-of-arrival estimation in massive MIMO," in *2017 IEEE International Conference on Acoustics, Speech and Signal Processing (ICASSP)*, pp. 3181–3185, New Orleans, LA, 2017.
- [33] P. Stoica, E. G. Larsson, and A. B. Gershman, "The stochastic CRB for array processing: a textbook derivation," *IEEE Signal Processing Letters*, vol. 8, no. 5, pp. 148–150, 2001.
- [34] C. Liu and P. P. Vaidyanathan, "Cramer-Rao bounds for coprime and other sparse arrays, which find more sources than sensors," *Digital Signal Processing*, vol. 61, pp. 43–61, 2017.
- [35] S. Qin, Y. D. Zhang, and M. G. Amin, "Generalized coprime array configurations for direction-of-arrival estimation," *IEEE Transactions on Signal Processing*, vol. 63, no. 6, pp. 1377–1390, 2015.